perforated electrode were investigated. The flow pattern of gas-solution mixture in a cell was complicated. It depended on the electrolytic current, but was almost independent of the perforation in the range more than 10%.

The reduced resistivity of a gas-solution mixture in a cell with the perforated electrode was a weak function of the electrode gap, but it increased with increasing distance from the cell bottom due to accumulation of bubbles depending on the depth. The terminal voltage of a cell with the perforated electrode was a linear function of the electrode gap in a wide range whereas the voltage of a narrow cell with the flat plate electrode rose with a decrease of the electrode gap less than 7 mm. However, reduction of the surface area by machining becomes a penalty of the perforated electrode when disengagement of gases from the solution is easy in wide channels. A desirable size of the gap between the perforated electrode and the counterelectrode was estimated to be 5-10 mm (see Fig. 4A).

Since the gas void fraction in the elecrolysis zone in a cell using the perforated electrode is low compared to cells having the solid plate electrode, the current distribution along the perforated electrode is relatively uniform, and is similar to that in a well-designed cell under natural circulation.

The perforation area is also an important factor for reducing the cell voltage and its components. The solution resistivity was almost independent of the perforation area more than 10%, while it increased quickly when the open area was insufficient for escape of gas-solution mixture. The overvoltage decreased with increase of perforation up to 10% because of reducing the surface coverage of the working electrode with gas bubbles. On the other hand, the overvoltage increased when the working area became small by machining. Consequently, a minimum cell voltage could be obtained by the perforated electrode in the range 5-15% open.

It was clarified that only a small compartment such as 5 mm thick of the back side of the electrode was required to provide the space for disengagement of gases from the electrolytic solution so as to keep the cell voltage low.

Acknowledgment

The study has been conducted under the financial support of Japan Soda Industry Association and Grant-in-Aid for Developmental Scientific Research, The Ministry of Education, Science and Culture, No. 485,203.

Manuscript submitted April 8, 1980; revised manuscript received July 23, 1980. This was Paper 385 presented at the St. Louis, Missouri, Meeting of the Society, May 6-11, 1980.

Any discussion of this paper will appear in a Discussion Section to be published in the December 1981 JOURNAL. All discussions for the December 1981 Discussion Section should be submitted by Aug. 1, 1981.

Publication costs of this article were assisted by Fumio Hine.

REFERENCES

1. F. Hine and K. Murakami, *This Journal*, **127**, 292 (1980).
2. J. Jorné and J. F. Louvar, *ibid.*, **127**, 298 (1980).
3. C. W. Tobias, *ibid.*, **106**, 833 (1959).
4. F. Hine, M. Yasuda, R. Nakamura, and T. Noda, *ibid.*, **122**, 1185 (1975).
5. F. Hine, S. Yoshizawa, and S. Okada, *ibid.*, **103**, 186 (1956).
6. F. Hine and T. Sugimoto, Paper 459 presented at The Electrochemical Society Meeting, Seattle, Washington, May 21-26, 1978.
7. L. Sigrist, O. Dossenbach, and N. Ibl, *J. Appl. Electrochem.*, **10**, 223 (1980).

An Electrochemical Model for Oxide Growth on Zircaloy-2

N. Ramasubramanian*

Atomic Energy of Canada Limited, Materials Science Branch, Chalk River Nuclear Laboratories, Chalk River, Ontario, Canada K0J 1J0

ABSTRACT

The kinetics of Zircaloy-2 oxidation were followed at 573 K in oxygen-free steam and dry air. At various stages during the oxidation polarization measurements were made in molten alkali nitrates and nitrite at 573 K. These measurements provided a comparison of the ionic conductivity of the zirconia and the electrical conductivity of the oxide on the intermetallics, grown in steam and air with those of the oxides grown in the molten salts. A model is proposed for thermal oxide growth on Zircaloy-2. During oxidation in steam, protons are conducted in the adsorbed water phase and reduced by the electron transport occurring at the conducting intermetallic sites. Thus, the oxidation behavior is similar to that in the molten salts, where nitronium and nitrosonium ions are reduced to complete the oxidation. The low rates of oxidation observed in air are attributed to a high resistance for the surface conduction of electrons, and the absence of a conduction and reduction step involving cationic species. Therefore, the rest potential is not lowered as effectively as that during oxidation in steam and the molten salts, in spite of the electron conduction at the intermetallic sites. The molten salts are suitable media for studying, in general, the mechanism of oxide growth on Zircaloy-2; the information obtained is relevant either directly or indirectly.

It is known that the metal-oxide interface, during oxide growth on zirconium and Zircaloy-2, is at a negative potential relative to the oxide-oxidation medium interface. This is demonstrated by the oxidation studies in various media, such as aqueous electrolyte solutions (1, 2), oxygen (3, 4), molten salt (5-7), and steam (8). The attainment of this negative rest potential is determined by the relative ease of transport of oxygen ions and electrons through the growing oxide. An electrochemical interpretation of the kinetics

* Electrochemical Society Active Member.
Key words: fused salts, polarization, charge, transport.

of oxide growth is therefore based on the ionic and electronic conductivities of the growing oxide and their variations, if any, with the oxide growth.

When oxidizing in air, oxygen, or steam, the poor conductivity of the oxidation medium makes the use of an auxiliary electrode, contacting the oxide surface, a necessary requirement for electrochemical measurements. Such *in situ* measurements have been reported using evaporated or sputtered platinum layers (4, 8) and lithium-doped nickel oxide powder (3). In these types of experiments difficulties in interpreting the data were usually associated with an ill-defined contact area and the unknown factor of the influence of the contacting electrode on the oxidation itself.

It was shown that molten alkali nitrates and nitrites are convenient and suitable media for studying the mechanism of oxide growth on zirconium and Zircaloy-2 when the oxidation is also carried out in the molten salt (7). Unlike the evaporated metal and powdered semiconducting contacts, the contact area in the molten salt was well defined. We were, therefore, interested in extending the electrochemical polarization measurements in the molten salt to study the oxidation behavior of zirconium alloys in steam and air. In the study reported here, we have oxidized Zircaloy-2 in steam and air at 573 K and carried out polarization measurements at 573 K in the molten nitrite and nitrates at various stages during the oxidation. A model for thermal oxide growth on Zircaloy-2, which is essentially Cox's model (9) modified to account for the observed dependence of oxidation rate on the medium of oxidation in the early stages, is proposed.

Experimental

The molten salt baths used, and the procedures for sample preparation and polarization measurements following oxidation have been described elsewhere (7). All oxidation and polarization were carried out at 573 K. Samples, paddle-shaped and ≈8 cm² in area, were oxidized in oxygen-free steam at atmospheric pressure and dry air. In the closed steam loop, presence of air was avoided by flushing with argon before start-up and keeping it bubbling through the condensed water which returned to the boiler. At various times during the oxidation, the samples were withdrawn, weighed, polarized successively in molten KNO_3-$NaNO_3$, $NaNO_2$-$NaNO_3$-KNO_3, and $NaNO_2$, weighed again, and returned to their appropriate medium (steam loop or furnace) for further oxidation. Prior to polarization, sufficient time, usually half an hour, was allowed for the attainment of steady potential following immersion of the oxidized sample in the molten salt. The potentials are quoted relative to an Ag/Ag^+ (0.07M in $NaNO_3$-KNO_3) reference. Only weight gain measurements were made with some control samples.

Results

Oxidation of Zircaloy-2 in steam and polarization in the molten nitrates and nitrite.—The rates of oxidation in steam at atmospheric pressure were generally faster than those in the molten nitrates and nitrite and dry air. The results are shown in Fig. 1 where the data obtained in the molten salts and dry air are included for the sake of comparison. After a period of oxidation in steam, when the samples were polarized in the three molten salt baths in turn, the changes in the weight gain caused by the polarizations were quite small. They decreased from ≈0.3 mg/dm² in the initial stages, 28 hr oxidation, to nondetectable amounts towards the final stages, 700 hr, of oxidation.

A set of polarization curves, obtained subsequent to a 28 hr oxidation in steam, is shown in Fig. 2. The anodic portions showed well-defined plateaus which were spaced fairly closely to each other, within a range of 1-2 μA. However, the cathodic portions showed large differences; the resistance to the cathodic

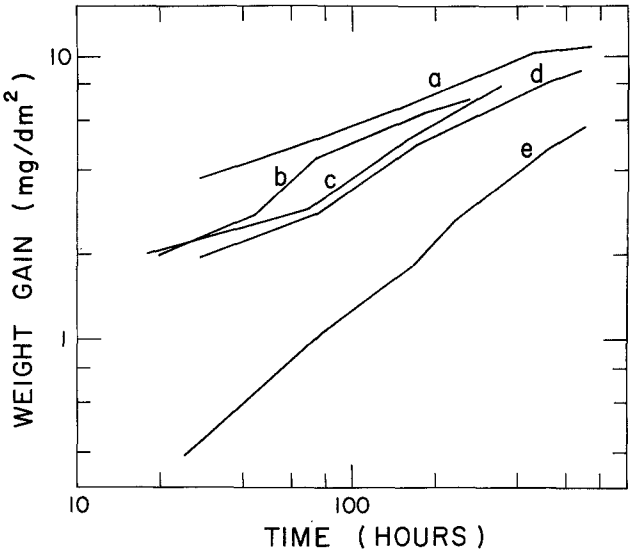

Fig. 1. Kinetics of oxidation of Zircaloy-2 at 573 K in: curve a, oxygen-free steam at atmospheric pressure; curve b, molten sodium nitrite; curve c, molten $NaNO_2$-$NaNO_3$-KNO_3; curve d, molten $NaNO_3$-KNO_3; and curve e, dry air.

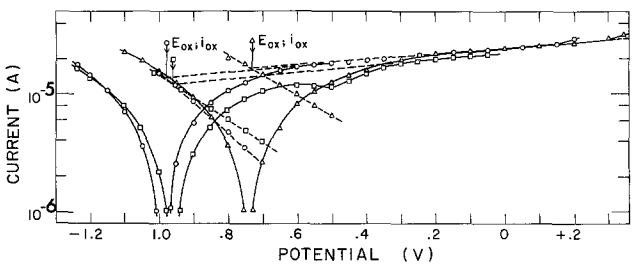

Fig. 2. Polarization curves traced at 573 K in △, binary nitrates; ○, ternary nitrates-nitrite; and □, sodium nitrite. Zircaloy-2 sample, oxidized 28 hr in steam at 573 K, had a weight gain of 3.8 mg/dm². Solid curves obtained experimentally, dashed curves obtained from analysis; E_{ox} — rest potential and i_{ox} — oxidation current.

current was much higher in the nitrite and ternary melts than in the binary melt. The oxidation currents (*i.e.*, the currents at the rest potentials on the extrapolated anodic plateaus) corresponded reasonably well with the rate of oxidation obtained from the kinetic data. Nearly identical oxidation currents were obtained by extrapolating the anodic plateaus in the linear plots of polarization current against applied potentials. Similar results were obtained from polarization measurements carried out after various periods of oxidation in steam. The cathodic portions of the polarization curves traced in the nitrite and ternary melts showed negative resistance regions; in the nitrite melt these were associated with a large shift by about 0.25V in the rest potential towards anodic values.

In Fig. 3(a), the rates of oxidation calculated from the oxidation currents and the kinetic data obtained in steam are compared at a series of weight gains. The agreement between the two sets of data is not as good as that reported previously for Zircaloy-2 when both the oxidation and polarization were done in the same melt (7). The differences between the rates calculated from the polarization data in the three melts, at any weight gain, were more than the differences between the polarization derived rate in one melt and the kinetic rate. However, all the data showed the same trend of a decreasing rate with increase in weight gain. The oxygen ionic conductance of zirconia, at any oxide thickness, was calculated as the ratio of the oxidation current, obtained from the polarization data, to the anodic shift in the rest potential from the immersion potential. Immersion

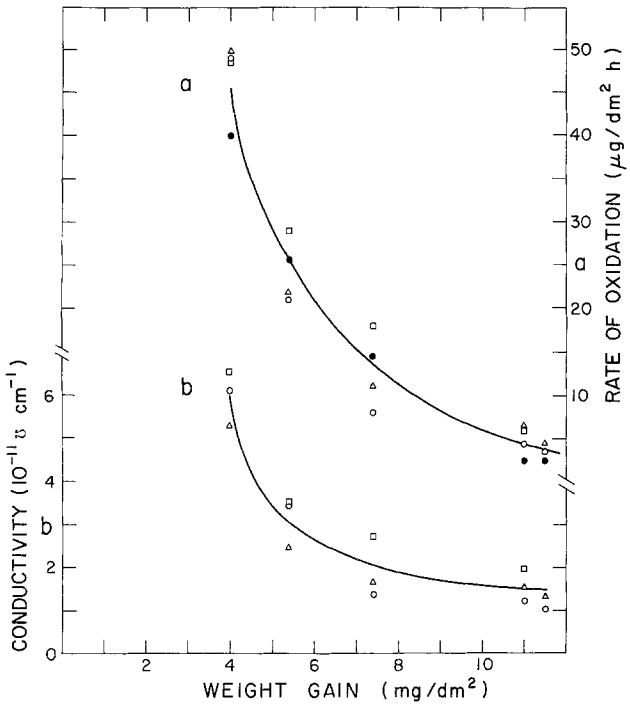

Fig. 3. Zircaloy-2 oxidized in steam at 573 K and polarized in the molten salts at the same temperature. Curve a, comparison of the oxidation rates obtained from the kinetic and polarization data. Polarization data from △, binary; ○, ternary; and □, nitrite melts; ●, kinetic data. Curve b, variation of the ionic conductivity with the weight gained; symbols refer to the same melts as in curve a.

potentials for Zircaloy-2 in the three melts at 573 K have already been reported (7); they varied from −1.8V in the binary and ternary melts to −1.6V in the nitrite. The ionic conductivities calculated are shown in Fig. 3(b) as a function of weight gain. The behavior is quite similar to that of the rate of oxidation shown in Fig. 3(a) and of the ionic conductivity of the oxide grown in the sodium nitrite melt reported elsewhere (7).

The variation of the resistance to cathodic current flow with time of oxidation is shown in Fig. 4. In the binary and ternary melts a systematic increase in the resistance was observed and the rest potentials were steady at ≈ −0.7 and −0.85V during most of the oxidation. The rest potentials obtained in the three melts are listed in Table I. When the results were compared with the oxides grown in the molten salts (7) the steam-grown films were found to be more resistive.

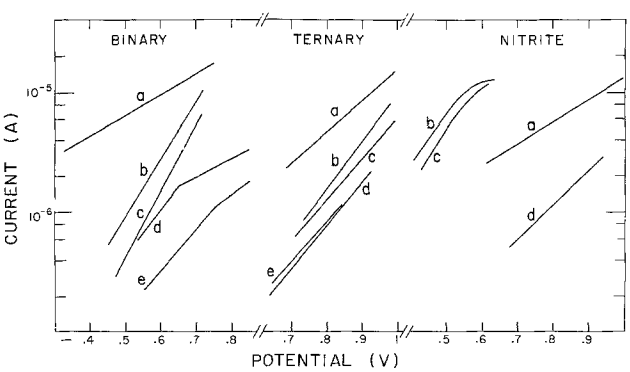

Fig. 4. Variation of the resistance to cathodic current flow at 573 K in the three molten salt baths with time of oxidation of Zircaloy-2 in steam at 573 K. Time of oxidation in hours: curve a, 28; curve b, 76; curve c, 172; curve d, 530; and curve e, 670.

Table I. Variation of the negative values of the rest potentials, obtained at 573 K in the three melts, with the time of oxidation of Zircaloy-2 in steam and dry air at 573 K

Time of oxidation (hr)	Oxidation in steam			Oxidation in dry air		
	Rest potentials (volts)			Rest potentials (volts)		
	Binary	Ternary	Nitrite	Binary	Ternary	Nitrite
28	0.73	0.97	0.96	0.93	1.21	0.60
76	0.67	0.93	0.53	0.70	1.08	0.57
172	0.66	0.86	0.50	0.70	0.98	0.53
316				0.61	0.97	0.52
503	0.70	0.85	0.86	0.61	0.95	0.49
670	0.79	0.83		0.53	0.62	

Oxidation of Zircaloy-2 in dry air and polarization measurements in molten nitrates and nitrite.—The rate of oxidation in dry air was much slower than those in the molten salts and steam. When the samples were polarized in the molten salts the resulting changes in the weight gain were very considerable, especially in the initial stages. These changes are shown in Fig. 5 where the kinetics of oxidation in dry air of a control sample are compared with those of another sample on which intermittent polarizations in the molten salts were carried out. The changes in the weight gain as a result of these immersions and polarizations in the melts are shown by the dashed portions. In the initial stages the weight gained during one set of polarizations, *i.e.*, in a total time of 5 hr of immersion and polarization in the three melts, was as much as that gained in 30 hr of oxidation in air. In the first 200 hr the weight gained as a result of three sets of immersions and polarizations, lasting nearly 18 hr, was more than half of the total weight gained.

In Fig. 6, the results are plotted on linear scales and the transfers made, from the dry air to the molten salts for polarization measurements and vice versa for continuing the oxidation in dry air, are shown by the horizontal dashed lines and are listed in alphabetical order. The direction of the arrows identifies the transfer made. The data for the control samples oxidized in air and the molten salts are shown by the solid curves; the curve for the latter is the average of the weights gained in the three melts. The data for the sample oxidized in air and polarized in the melts at various times during the oxidation are shown by the solid circles. When a transfer was made, *e.g.*, from the air to the molten salts, the location corres-

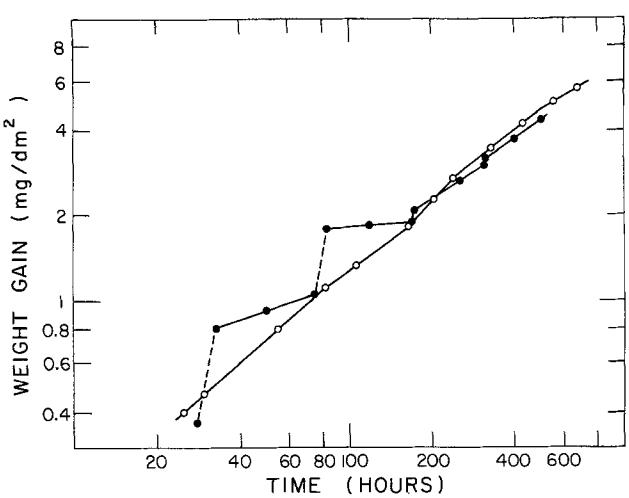

Fig. 5. Effect of immersion in the molten salts on the weight gained by Zircaloy-2 during oxidation in dry air at 573 K. ○, control sample oxidized without immersion in the molten salts and ●, sample oxidized with intermittent immersions in the molten salts at 573 K for polarizations. Solid curves—weight gained in air and dashed curves—weight gained in the salts.

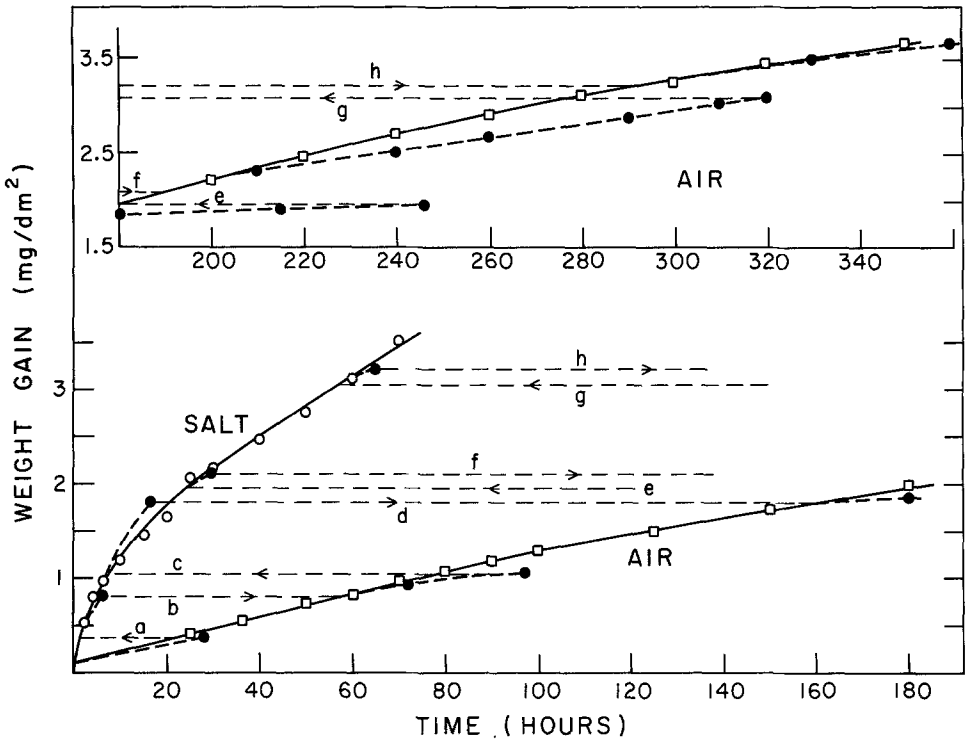

Fig. 6. Oxidation occurring, in the molten salts, during the polarization measurements on a Zircaloy-2 sample oxidized in dry air. Comparison of the kinetics of oxidation with those of the control samples oxidizing only in air or the molten salts. ○, control oxidizing in the molten salts at 573 K; average of the weights gained in the three melts; □, control oxidizing in dry air at 573 K; and ●, oxidized in dry air at 573 K and polarized in the three melts at 573 K. a, c, e, and g—transfers to the salts and b, d, f, and h—transfers to dry air.

ponding to the weight gain at the time of transfer is identified on the oxidation curve of the control sample in the melts and further weight gain is plotted from this location. A similar procedure is followed when the sample was returned to the air for further oxidation. It is readily seen that in all the transfers, excepting d, the kinetics of oxidation of the sample in air and the molten salts follow closely the kinetics of oxidation of the control samples in the respective medium. Therefore, the oxidation behavior of a sample oxidized both in dry air and in the molten salts, the latter resulting from the polarization measurements, is the same as that of an oxide of equivalent thickness growing only in air or the molten salts.

In order to separate the contributions to the weight gain changes in the melts caused by the immersion from those caused by anodic polarization, the following types of measurements were carried out with pairs of samples oxidized in dry air for various times. When a pair of samples oxidized for the same length of time was immersed in a melt, one of the pair was left unpolarized while the other was polarized to give current-voltage data. The changes in the weights gained by both were compared at the end of the experiment. When the initial weight gain in air was $\approx$0.4 mg/dm^2, immersion in the molten salt alone was responsible for $\approx$80% of the increase in weight gain and anodic oxidation (resulting from the polarization) contributed to the remaining 20% increase. However, the latter decreased to $\leq$10% at a total weight gain of $\approx$1 mg/dm^2 and was negligibly small at higher weight gains.

A set of polarization curves in the three melts following a 28 hr oxidation in air is shown in Fig. 7. The anodic plateaus were well defined and placed one below the other in the same order as the polarizations; the spread amongst the plateaus was about 10 μA. With increasing oxidation, the anodic plateaus were still well defined, but the spread amongst them decreased to 1-2 μA. The negative values of the rest potentials varied as sodium nitrite < binary nitrates < ternary nitrates and nitrite; these are listed in Table I. Negative resistance regions were observed in the cathodic portions of the polarization curves traced in the two nitrite-containing melts.

When the anodic plateaus were extrapolated, the oxidation currents obtained at the rest potentials were too high to correspond to the rates of oxidation in air calculated from the kinetic data. However, the oxidation currents from the polarization data agreed well with the changes in the weight gain resulting from immersion and polarization in the melts, *i.e.*, with the rates evaluated from the dashed portions in Fig. 5. These rates were also found to be comparable to the rates obtained in molten salt oxidation (7).

The results are shown in Fig. 8(a) where the rates of oxidation calculated from the polarizations, the oxidation kinetics in air, and the weight gain changes due to immersion in the melts are compared at different weight gains. Because the weight gain changed considerably due to immersion in the salt, the total weight gained by the sample at the end of a polarization step, rather than that due to oxidation in air, was used in plotting the data. At any weight gain the difference between the rates, calculated from the polarization data obtained in the ternary eutectic and the sodium nitrite melt, was rather large. In Fig. 8(b) the variation of the ionic conductivity of the oxide with the weight gain is shown. The conductivities and their variation in behavior were found to be similar to those reported for oxides grown in the three melts (7). When the results from the polarization data are compared the rate of oxidation decreased initially, up to a weight gain of $\approx$2.5 mg/dm^2, and the ionic conductivity stayed

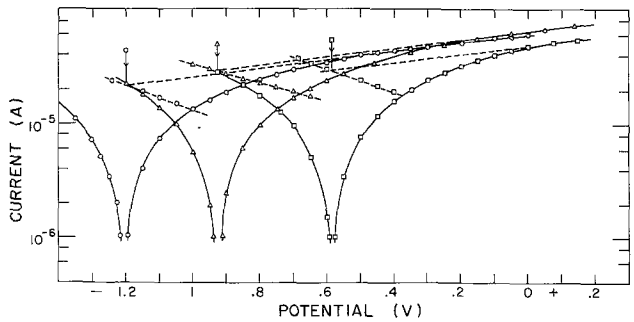

Fig. 7. Polarization curves traced at 573 K in △, binary nitrates; ○, ternary nitrates-nitrite; and □, sodium nitrite. Zircaloy-2 sample oxidized 28 hr in air at 573 K. Solid curves obtained experimentally, dashed curves obtained from analysis; arrows locate rest potentials and oxidation currents.

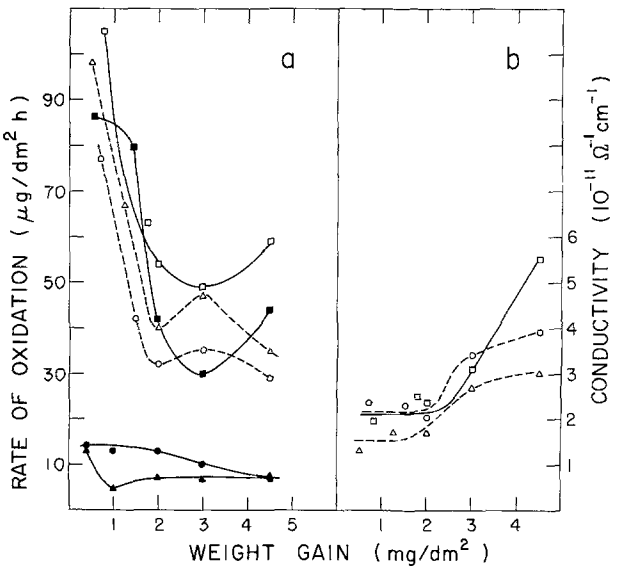

Fig. 8. Zircaloy-2 oxidized in dry air at 573 K and polarized in the three melts at the same temperature. (a) Comparison of the rates of oxidation calculated from the polarization with those obtained from the kinetic data in air and the weight gained in the salt. Polarization data: △, binary nitrates; ○, ternary nitrates-nitrite; and □, sodium nitrite. Kinetic data in air: ●, nonpolarized sample and ▲, sample intermittently polarized in the three melts. ■, rate from the weight gained due to immersion in the salt. (b) variation of the ionic conductivity with the weight gained; symbols refer to the same melts as in (a).

nearly steady at 2×10^{-11} Ω^{-1} cm^{-1}. With further increase in weight gain the rate of oxidation and the ionic conductivity increased; in the case of the binary and ternary melts the rate of oxidation showed a maximum and this corresponded to an inflection in the conductivity curve.

The resistance to cathodic current flow as a function of weight gain is shown in Fig. 9. The rest potential decreased with increasing oxidation; the resistance in the three melts varied as sodium nitrite < binary nitrates < ternary nitrate-nitrite. At comparable weight gains, the air-grown films were found to be more conducting than films grown in steam and less conducting than films grown in the molten salts (7).

Discussion

Anodic and cathodic processes during thermal oxide growth on Zircaloy-2.—In a discussion about the relation between the type of rate law obeyed, during the thermal oxidation of zirconium and Zircaloy-2 at 473-573 K, and the oxide thickness it was concluded that the anodic process is controlled by a field dependent rate-determining process within the oxide film and that the weak field approximation of the equation usually employed for anodic oxide growth is applicable (1). This was confirmed by the results

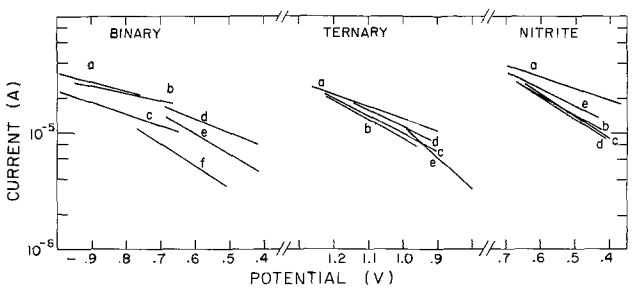

Fig. 9. Variation of the resistance to cathodic current flow at 573 K in the three molten salt baths with time of oxidation of Zircaloy-2 in air at 573 K. Time of oxidation in hours: a, 28; b, 76; c, 172; d, 316; e, 503; and f, 670.

obtained in the oxidation and polarization experiments in the molten salts at 573 K; it was shown that the potentials corresponding to the linear anodic plateaus in the polarization curves were essentially across the zirconium oxide and the anodic process of oxygen ion transport was determined by the ionic conductivity of the oxide (7).

Bacarella and Sutton had interpreted the cathodic process on the basis of a dual barrier model; the zirconium oxide was assumed to be a semiconductor having an electron transfer coefficient close to unity; a part of the potential drop was considered to be across this oxide barrier and the remaining at the oxide-solution interface controlling a charge transfer reaction (1). However, it has recently been shown that when the zirconia thickness is less than the average size of the intermetallic precipitates in the alloy, the electron transport, completing the oxidation, occurs predominantly at the oxidized zirconium-iron intermetallic precipitates (5, 6). The composition of the oxides grown on these second phase precipitates and its variation with the temperature and extent of oxidation have not been investigated in detail. In addition, the cathodic portions of the analyzed polarization curves generally showed two "Tafel" regions; the data could also be fitted to, sometimes better than a Tafel relation, a Schottky type of emission process. The variation of the resistance to cathodic current flow with increasing oxidation was found to depend on the medium in which the alloy was oxidized. Therefore, in the absence of definitive experimental evidence, of the fit of the data to a single type of electron transport mechanism, the cathodic process is simply considered to be determined by the conductivity of the oxide grown on the second phase intermetallic precipitates.

Oxidized Zircaloy-2 sample immersed in molten alkali nitrates, nitrites, and their eutectics.—The reactions occurring in molten alkali nitrates, nitrites, and their eutectics and their relevance to the mechanism of oxide growth on Zircaloy-2 in these melts have been discussed elsewhere (7). The oxide thicknesses investigated in the present study are well below 1 μm (equivalent weight gain is $\approx$15 mg/dm^2), the average size of the intermetallics. Therefore, irrespective of which medium the alloy was oxidized in, when it is immersed in the molten salt it can be expected to acquire a rest potential determined by the ionic conductivity of the zirconia and the electronic conductivity of the oxide grown on the intermetallic precipitates. The kinetics of oxidation of a Zircaloy-2 sample, oxidized in steam or aqueous solutions or molten salts and intermittently polarized in the molten salts, is found to be nearly identical to that of a control sample which had not been polarized. It can be concluded therefore, that immersion and polarization in the molten salts are not affecting the conduction properties of the zirconia and the oxide on the intermetallic precipitates and information on these oxide conductivities can be obtained from the polarization data. This is the basis for exploring the possibility of using molten alkali nitrates and nitrites as polarization media for studying oxide growth in other media such as air and steam.

However, the reactions on the alloy and the intermetallics at the oxide-molten salt interface would be different from those that occurred at the oxide-oxidation medium interface during the oxidation. Therefore, the polarization data obtained in the molten salts might correspond more closely to the oxidation behavior of a preoxidized sample in the salt than to the previous history of oxidation in another medium. But, apart from these differences (due to the different interfacial reactions at the oxide surface during oxidation and polarization) the data obtained in the molten salts should provide information on the variation of the oxide conductivities with increase in oxidation,

and a comparison amongst the oxides grown in various media. Such information is important in interpreting the mechanism of oxide growth.

Oxidation in steam.—Following a period of oxidation in steam, when a sample was polarized in the three melts it was observed that the anodic plateaus in the polarization curves were quite close to each other. As the plateaus are identified with the oxygen ionic transport in the zirconia (7, 9) this observation indicates that the ionic conductivity of the zirconia had remained the same during the polarization. But there were variations in the values of the ionic conductivity calculated, at any weight gain, as shown in Fig. 3(b). These might be due to small differences in the measured anodic currents resulting from the repeated polarizations within a short time and to some extent also due to the slightly different values of the measured immersion potentials used for the three melts. Unlike the ionic currents, the cathodic reduction currents in the three melts showed large variations indicating that the resistance of the same oxide film, grown in steam on the intermetallics, was different in the three melts. The interpretation is that the surface reactions involved and their current-voltage characteristics are different in the three melts; *viz.*, reduction of NO_2^+ in the binary nitrates, NO^+ in the nitrite, and possibly both of these species in the ternary nitrate-nitrite melt.

Thus, when the results from the polarization curves are correlated with the reactions occurring during the oxidation in steam, the ion transport can be expected to be in better agreement than the electron transport. The ion transport, determined by the conductivity along the crystallite boundaries, occurs through the same oxide during oxidation in steam and polarization in the three melts. The ionic conductivities shown in Fig. 3(b) are thus characteristic of the oxide grown in steam and the same as those that existed during the oxidation. The electron transport, on the other hand, is not only related to different reactions in the three melts during polarization but is also associated with a completely different reaction, the reduction of protons to hydrogen, during the oxidation in steam. Thus, the different rest potentials and oxidation currents measured in the three melts (subsequent to a period of oxidation in steam) and the differences in the oxidation rates calculated from the polarization data in the three melts and the kinetic data in steam (at a weight gain) are to be attributed mainly to the different cathodic reduction reactions. For the same reason the rest potential during the oxidation in steam would have been different from those observed during polarization.

In spite of only a reasonable agreement between the rates of oxidation calculated from the polarization and kinetic data, it can be stated that the polarization data do reflect changes in the ionic conductivity of the oxide grown in steam and also changes in the rate of oxidation in steam with the weight gain. The same trend is seen in the rates of oxidation derived from the kinetics as is seen in the calculated ionic conductivities [*cf.* Fig. 3(a)]. The ionic conductivity of the steam grown oxide (as revealed by polarization) is slightly higher than but close to that of the oxide grown in the nitrite melt (7). The kinetics of oxidation in steam are faster than in the molten salts to begin with, but at a weight gain >4 mg/dm^2 the kinetics become comparable to those in the nitrite melt. This similarity between oxidation in steam and molten sodium nitrite might be attributed to a higher water content in the nitrite melt (present as an impurity) than in the binary and ternary eutectics (7). However, a high ionic conductivity for the oxide grown in steam is revealed by polarization in all the three melts. The similarity to oxidation in the nitrite melt then suggests that the current-voltage characteristics of the cathodic reduction of protons to hydrogen during steam oxidation are similar to those of the reduction reactions occurring in the nitrite melt. Therefore, it can be concluded that molten alkali nitrates, nitrites, and their eutectics, in general, are suitable polarization media for studying the oxide growth on Zircaloy-2 in steam.

Oxidation in dry air.—The behavior of samples oxidized in dry air, when immersed in the molten salts, was very different from that of the steam-oxidized samples in that considerable additional oxidation occurred in the salt. The kinetic and polarization characteristics of this additional oxidation are seen to be nearly the same as those of an oxide of equivalent thickness grown in the molten salts. Therefore, it has to be concluded that the ionic conductivity of the zirconia and the electronic conductivity of the oxide on the intermetallics grown in air are not very different from those of the oxides grown in the molten salts. This is confirmed by the ionic conductivities and the resistances to cathodic current flow calculated from the polarization data.

There was no agreement between the rates of oxidation calculated from the polarization and kinetic data at any weight gain; the rates derived from the polarization data, however, corresponded to the additional oxidation occurring in the melts. The variation in the rates of oxidation, calculated from the polarization data obtained in the three melts, could also be related to the resistance of the oxide on the intermetallics to the cathodic current and the rest potentials. In the ternary melt the latter were high and the oxidation rate was low; in the nitrite melt, the resistance and the rest potentials were low and the oxidation rate was high. Therefore, the behavior of the air-grown oxide in the molten salts represents the oxidation occurring in the salt during immersion rather than the previous history of air oxidation. The polarization data are, therefore, not relevant to air oxidation.

The near linearity of the oxidation rate in the initial stages, of the control sample, suggests that the oxidation in dry air is controlled by a surface reaction. Similar low and near linear rates were observed in the case of samples oxidized in air and polarized intermittently in the molten salts. These results indicate that in spite of the electrical conduction properties of the oxides grown in air and/or the molten salts being basically the same the oxidation in dry air proceeds at a slower rate. As will be discussed later, this is to be attributed to a basic change in the mechanism related to the conduction properties of the oxide surface. Therefore, inferences regarding oxide growth in air could be drawn by comparing the polarization behavior of the oxide with those grown in steam and the molten salts.

Model for thermal oxide growth on Zircaloy-2.—The kinetics of oxidation in steam, though resulting in a faster rate of oxidation than in the molten salts, are seen to be close to those in the nitrite melt at weight gains ≥ 4 mg/dm^2. The mechanism of oxide growth in steam is, therefore, likely to bear some analogy to that in the molten salts (7). As the oxygen ions for the oxidation have to come from the water molecules the cathodic reaction completing the oxidation has to be the reduction of protons. The mechanism, generally proposed, for oxidation in aqueous electrolyte solutions is the reduction of water to hydroxyl ions (mostly localized at the intermetallic sites) and the reaction of a pair of hydroxyl ions from the solution on the zirconia surface producing oxygen ions and water (2). If the same scheme is to be applied for oxidation in steam, the hydroxyl ions produced at the intermetallic sites have to be transported by surface conduction to reaction areas on the zirconia. But the mobility of protons is considered to be generally faster than that of the hydroxyl ions (10); and during the initial stages of oxide growth in steam and aqueous solutions a considerable fraction of the hydrogen re-

leased is absorbed by the alloy (9). Therefore, equally well the oxygen ions could be extracted from the adsorbed water by the anion vacancy emerging on the zirconia surface and the protons released transported to the intermetallic sites and/or the alloy-oxide interface for reduction.

The model for oxide growth is the same as that proposed by Cox (9) and adapted for oxidation in molten salts (7). Oxygen ions, produced by a dissociation step, are transported along the zirconia crystallite boundaries by diffusion and the protons, transported by surface conduction, are reduced at the intermetallic sites. This latter reaction is analogous to the reduction of NO_2^+ and NO^+ during oxidation in the molten salts. The electronic conductivity of the doped oxide grown on the intermetallics maintains the rest potential at moderately low negative values. When the polarization data obtained in the molten nitrite are compared, the resistance of the oxide on the intermetallics grown in steam is higher than that grown in the molten nitrite. But the ionic conductivity of the zirconia grown in steam is higher than that grown in the nitrite; the compensating effect due to the ionic conductivity leads to faster oxidation in steam compared to that in the molten nitrite.

When the kinetics of oxidation in steam, molten salts, and air are compared the characteristics of the last are seen to be very different from those of the first two. The rate in air is about an order of magnitude less than that in the molten salts at a low weight gain of $\approx$1 mg/dm^2 and is about four times less than those in steam and molten salts at high weight gains up to $\approx$5 mg/dm^2. It is almost linear up to a weight gain of $\approx$2 mg/dm^2. When the air-oxidized sample is immersed in the molten salts, it oxidizes at an increased rate corresponding to the rate of oxidation of a control sample oxidizing in the melts. However, the rate returns to low values, similar to those of a control sample oxidizing in air, when further oxidation is continued in air. Therefore, there is a basic change in the mechanism of oxidation when a sample is transferred from dry air to molten salt and vice versa.

The transport of oxygen ions along crystallite boundaries, is nearly the same in various oxidation media due to nucleation and crystallite growth occurring at the alloy-oxide interface (9). The zirconia crystallites are reported to occupy almost 100% of the oxide volume by the time a thickness of $\approx$0.2 μm is reached. Therefore, major changes in the ionic conductivity of the oxide, imparted by the oxidation medium and associated with crystallite size, impurity incorporation, and surface structures, can be expected to occur during the initial stages of thin film growth. It is observed (*c.f.* Fig. 8) that the ionic conductivity of the air-grown oxide, subsequent to immersions and polarizations in the molten salts, and its variation with the total weight gained are comparable to those of the oxides grown in the molten salts (7). Therefore, the different oxidation behavior observed in dry air and the molten salts is not associated with the oxygen ion conduction in the growing zirconia. The cathodic step in air oxidation is the reduction of oxygen and this reaction has to occur on the zirconia surface near an emerging anion vacancy. The electrons could be transported from the intermetallics by conduction along the p-levels of the chemisorbed oxygen. This surface conduction and/or the reduction of oxygen must be then rate limiting.

Moreover, during oxidation in dry air, conduction and reduction of a cationic species are not involved. Therefore, lowering of the resistance of the alloy-oxide composite may not be as effective as that during oxidation in steam and the molten salts and consequently the rest potential could be highly negative. The rest potential at which the ionic current is equivalent to the rate of oxidation in air can be estimated as $\sim$ -1.6V from the extrapolated anodic plateaus in the polarization curves. Such a highly negative rest potential, combined with a low rate of oxide growth, can be expected to contribute to a bulk electron current through the zirconia. In the initial stages, when the oxide is a few hundred angstroms thick, this might be an emission current, which may become space charge limited with increase in oxide thickness. The contribution from these bulk currents would, however, decrease with increasing weight gain.

Dawson *et al.* reported that the oxidation behavior of chemically polished Zircaloy-2 in oxygen at 573-633 K was complex (11). A change from a near linear to a near parabolic rate is also observed in the present study. Such variations can be interpreted as a reflection of the changes occurring in the electron transport. Initially the rate is linear due to the limited rate of oxygen reduction at the surface determined by the bulk emission current. The rate then decreases due to the buildup of electronic space charge which affects both the ionic and electronic transport and changes again at a higher oxide thickness when the bulk electron current is negligible and localized transport at the intermetallics combined with the surface conduction becomes limiting. When the air-oxidized sample is immersed in the molten salt for polarization the situation is changed completely. The reduction of nitronium and/or nitrosonium ions facilitated by the electron transport at the intermetallics, moves the rest potential to low negative values and any space charge or surface resistance effect on the oxidation rate is minimized; the alloy oxidizes at a rate near to that expected for an oxide of equal thickness in the molten salt.

In their model, Brown and Walton (2) proposed a surface barrier in addition to the growing oxide film barrier for the anodic current. This surface barrier was supposed to control an ionic reaction, not necessarily a rate-determining step, such as dehydroxylation in their experiments. It is seen from the results reported here that the role played by a surface barrier, if it exists, is a very minor one in the oxidation of Zircaloy-2. The interfacial reactions at the oxide-oxidizing medium are all different in different media. But in all media the rate of oxidation is determined by a combination of factors, such as ionic conductivity of the zirconia, electronic conductivity of the oxide on intermetallics, reduction of cationic species in the medium, and the bulk electronic conductivity of zirconia. The surface conduction properties of the zirconia associated with the reduction reactions play a more major role, than a surface barrier, in determining the oxidation of Zircaloy-2. In a similar manner, it cannot be said that either the ion transport or the electron transport is rate controlling (3); because ionic and electronic transport are occurring through different oxide systems, obey different current-voltage relations, and have to be coupled. It can be stated, however, that the anodic half of the oxidation (the oxygen ion transport) is less affected by changes in oxidation medium than the cathodic half. This effect is most evident when oxidation in a conducting medium is compared with that in a nonconducting medium.

Conclusions

Polarization measurements in molten alkali nitrates, nitrites, and their eutectics, on Zircaloy-2 samples oxidized in steam or dry air provide information on the variation of the ionic conductivity of zirconia and the electronic conductivity of the oxide grown on the intermetallics with increasing oxidation. The anodic part of the polarization data is directly relevant to the oxygen ion transport occurring during the oxidation; whereas the cathodic part of the polarization data has no direct correlation to the reduction reactions occurring during the oxidation. Thus, the differences in the oxidation rates calculated from the

polarization and kinetic data arise mainly from the different cathodic reactions involved.

A model for thermal oxide growth at ≤ 1 μm in thickness is proposed, based on the kinetic and polarization data.

1. When oxidizing in steam, the reduction of the protons released is assisted by their surface conduction in the adsorbed water phase on the zirconia surface and the electron transport at the intermetallic sites. Therefore, the rest potential stays at low negative values and the oxidation proceeds at a fast rate comparable to that in the molten salts.

2. In dry air, the oxidation proceeds at a much slower rate than in steam and the molten salts. The electrical conduction properties of the oxides grown in air, however, are similar to those of the oxides grown in the molten salts. Therefore, the low rates of oxidation in air are attributed to a highly negative rest potential on the alloy brought about by a high resistance for the surface conduction of electrons and the absence of a reduction step involving cationic species. The rate of oxidation, initially linear, is controlled by the reduction of oxygen at the surface; then the rate changes due to the buildup of an electronic space charge in the oxide and control by the combination of electron conductivity at the intermetallics and surface conduction.

Acknowledgments

The author wishes to acknowledge the many helpful discussions he had with Dr. B. Cox and the assistance offered by Mr. V. C. Ling in sample preparation.

Manuscript submitted Jan. 5, 1980; revised manuscript received May 20, 1980. This was Paper 63 presented at the Seattle, Washington, Meeting of the Society, May 21-26, 1978.

Any discussion of this paper will appear in a Discussion Section to be published in the December 1981 JOURNAL. All discussions for the December 1981 Discussion Section should be submitted by Aug. 1, 1981.

Publication costs of this article were assisted by Atomic Energy of Canada Limited.

REFERENCES

1. A. L. Bacarella and A. L. Sutton, *This Journal*, **112**, 546 (1965).
2. M. L. Brown and G. N. Walton, *J. Nucl. Mater.*, **66**, 44 (1977).
3. D. H. Bradhurst, J. E. Draley, and C. J. Van Drunen, *This Journal*, **112**, 1171 (1965).
4. J. H. Eriksen and K. Hauffe, *Z. Phys. Chem. N.F.*, **59**, 332 (1968).
5. B. Cox, *J. Nucl. Mater.*, **31**, 48 (1969).
6. N. Ramasubramanian, *ibid.*, **55**, 134 (1975).
7. N. Ramasubramanian, *This Journal*, **127**, 2566 (1980).
8. A. W. Urquhart, D. A. Vermilyea, and W. A. Rocco, *ibid.*, **125**, 199 (1978).
9. B. Cox, in "Advances in Corrosion Science and Technology," Vol. 5, M. G. Fontana and R. W. Staehle, Editors, pp. 301-311 and 343-361, Plenum Press, New York (1976).
10. G. C. Pimentel and A. L. McClellan, "The Hydrogen Bond," p. 31 and 253, W. H. Freeman and Company, San Francisco, California (1960).
11. J. K. Dawson, U. C. Baugh, and J. F. White, in "Zirconium and Its Alloys," J. P. Pemsler, E. C. W. Perryman, and W. W. Smeltzer, Editors, p. 137, The Electrochemical Society Softbound Proceedings Series, New York (1966).

High Oxygen Ion Conduction in Sintered Oxides of the Bi_2O_3-Dy_2O_3 System

M. J. Verkerk and A. J. Burggraaf

Department of Inorganic Materials Science, Twente University of Technology, 7500 AE Enschede, The Netherlands

ABSTRACT

The phase diagram of the Bi_2O_3-Dy_2O_3 system was investigated. A monophasic fcc structure was stabilized for samples containing 28.5-50.0 mole percent (m/o) Dy_2O_3. Above and below this concentration range polyphasic regions appear. The fcc phase showed high oxygen ion conduction. The ionic transference number is equal to one for specimens containing 28.5-40.0 m/o Dy_2O_3, whereas an electronic component is introduced at low temperatures for specimens containing 50.0 m/o Dy_2O_3. The conductivity of $(Bi_2O_3)_{0.715}(Dy_2O_3)_{0.285}$ is 0.71 $\Omega^{-1}m^{-1}$ and 14.4 $\Omega^{-1}m^{-1}$ at 773 and 973 K, respectively. Relations were found between the ionic radius, the conductivity, and the minimum concentration of lanthanide necessary to stabilize the fcc phase. It is concluded that the highest ionic conductivity will be found in the system Bi_2O_3-Er_2O_3 or Bi_2O_3-Tm_2O_3. From a study of relations between the activation energy, log σ_0 and the composition it is concluded that two conductivity mechanisms play a role.

Recently Harwig investigated the electrical and structural properties of Bi_2O_3 (1-5). At room temperature the monoclinic α-phase is stable and the conductivity is predominantly electronic. On heating to 1002 K the oxide transforms to the face centered cubic (fcc) δ-phase, which is stable up to the melting point at 1097 K. In the δ-phase the electrical conductivity is about 100 $\Omega^{-1}m^{-1}$ and varies little with temperature. The ionic transport number is equal to one (6). On cooling this highly conductive phase may be extended to 923 K, where it transforms into the tetragonal β-phase or to 912 K where it transforms into the body-centered cubic (bcc) γ-phase. These phase transformations are accompanied by sudden volume changes which cause deterioration of the mechanical properties of the material. The conductivity in the β- and γ-phase is mainly ionic and about three orders of magnitude lower than in the δ-phase.

The temperature range at which this material can be used as a solid electrolyte can be extended by substituting Bi_2O_3. The region of highly ionic conductive δ-phase can be extended to room temperature by intro-

Key words: ionic conductor, solid electrolyte, bismuth oxide, lanthanide oxide, phase relations.